Minerals Engineering 163 (2021) 106751

Contents lists available at ScienceDirect

Minerals Engineering

journal homepage: www.elsevier.com/locate/mineng

Extraction of Nb and Ta from a coltan ore from South Kivu in the DRC by alkaline roasting – thermodynamic and kinetic aspects

A. Shikika [a,b], F. Muvundja [b], M.C. Mugumaoderha [c,d], St. Gaydardzhiev [a,*]

[a] GeMMe-Mineral Processing and Recycling, University of Liège, Allée de la Decouverte 9, Sart Tilman, 4000 Liege, Belgium
[b] Dept. of Physical Chemistry, Higher Pedagogical Institute of Bukavu, Av. Kibombo 32, Bukavu, The Democratic Republic of the Congo
[c] Dept. of Physics and Technology, Higher Pedagogical Institute of Bukavu, Av. Kibombo 32, Bukavu, The Democratic Republic of the Congo
[d] Dept. of Physics, University of Namur, 5000 Namur, Belgium

ARTICLE INFO

Keywords:
Coltan
Roasting
Niobium
Tantalum
Kinetic models
Water leaching

ABSTRACT

An alkaline roasting of a coltan bearing ore from the Numbi deposit (South Kivu, the DRC) was investigated with particular focus on the extraction kinetics of Ta and Nb. Isothermal roasting experiments were carried out to study the effects from KOH to ore mass ratio, particle size and roasting temperature on the degree of Ta and Nb recoveries. The roasting efficiency was found to be affected by all the parameters being studied with their optimal values being found as following: particle size range +75–45 μm, KOH to ore ratio 3/1, roasting temperature 550 °C and roasting duration of 1 h. Under these conditions, 80% of Ta and 87% of Nb were recovered from the ore. The kinetic data analysis by different kinetic models indicated that the caustic potash roasting of the Numbi coltan ore is governed by a chemical reaction at particle surface. The apparent activation energies for Ta and Nb were estimated as 40.9 and 46.1 $kJ.mol^{-1}$ respectively. The obtained results demonstrated that it is possible to bring Ta and Nb into solution without using hydrofluoric acid and deliver a pregnant leach solution (PLS) suitable for downstream treatment.

1. Introduction

The recent developments in advanced technologies, especially in the field of telecommunications, steel making, aerospace and nuclear energy have contributed to a drastic raise in the demand of strategic metals such as Ta and Nb and thus bringing pressure on extraction of columbo-tantalite (coltan) natural resources. The Democratic Republic of the Congo (DRC) holds the largest African reserves of coltan mineral resources (Hayes and Bruge, 2003; Mantz, 2008), with the majority of coltan deposits being located in the Eastern DRC, particularly around the Kivu provinces in the Kibaran belt. The mining activities are typically small scale artisanal ones targeting pegmatite and alluvial deposits. Recently, access to these resources was taken over by armed groups backgrounded by illegal distribution channels established in the region (Mantz, 2008; Moran et al., 2014, Wakenge, 2018). As a result, these proven coltan resources rarely benefit the social and economic development of the country. Hayes and Bruge (2003) reported on how coltan mining industry can support the development of the DRC economy, notably through a sustainable extraction of the value-added tantalum (Ta) and niobium (Nb) and traceable and transparent value chains.

The extraction of Ta and Nb from coltan reserves involves various processes, however frequently operated under highly aggressive conditions. The most common routes are based on the use of hydrofluoric acid (Htwe and Lwin, 2008) and alkaline agents (Zhou et al., 2005a, 2005b; Wang et al., 2009; El Hazek et al., 2019), and chlorination as well (Gaballah et al., 1997; Brocchi and Moura, 2008). Another approach of ore selective dissolution has been proposed by Allain et al. (2019) to produce a $(Ta, Nb)_2O_5$ concentrate, however without Ta and Nb separation. A hydrofluoric acid doped by sulphuric acid is often used on an industrial scale to directly leach Ta-Nb ores. However, the major drawback of this process lies in the difficulties in processing low-grade ores, and especially in the harmful effects provoked by the HF. During hydrofluoric acid leaching, about 6–7% of gaseous HF are released and wastewaters containing fluoride ions are generated (Agulyansky, 2004). The treatment of these effluents renders the process complicated, and the need to handle HF-based pollution presents a major environmental and economic challenge for the Ta-Nb extractive industries.

Over the past decades, the alkaline route has attracted reasonable attention in processing of low grade ores. The process could be practiced under two options, namely as direct leaching of the Ta-Nb ores and

* Corresponding author.
E-mail address: s.gaydardzhiev@uliege.be (St. Gaydardzhiev).

https://doi.org/10.1016/j.mineng.2020.106751
Received 30 July 2020; Received in revised form 24 November 2020; Accepted 19 December 2020

Table 1
Composition of the studied raw coltan ore as determined by an XRF analysis.

Oxide	SnO_2	SiO_2	Al_2O_3	Ta_2O_5	Fe_2O_3	Nb_2O_5	TiO_2	MnO	CaO
Content, %	33.00	19.80	11.80	11.10	7.62	5.02	4.83	2.14	1.79
Oxide	MgO	PbO	P_2O_5	CeO_2	Na_2O	WO_3	La_2O_3	Nd_2O_3	
Content, %	1.43	0.244	0.136	0.343	0.148	0.233	0.231	0.135	

through an alkaline roasting coupled to water leaching. The latter option is proven as an advantageous one since it consumes less alkaline reagents and is leading to high metallurgical recoveries of Ta and Nb (Wang et al., 2009; Yang et al., 2013). In this process, caustic potash is commonly used as roasting agent for generating water soluble niobates and tantalates. The overall roasting reaction could be represented as follows (Wang et al., 2009; Berhe et al., 2018):

$$(Fe, Mn)(Ta, Nb)_2O_6 + 6KOH \rightarrow 2K_3(Ta, Nb)O_4 + (Fe, Mn)O + 3H_2O \quad (1)$$

Previous studies (Wang et al., 2009, 2010; Berhe et al., 2018), have shown, that based on the roasting conditions, formation of undesirable compounds may take place as of the reaction below:

$$(Fe, Mn)(Ta, Nb)_2O_6 + 2KOH \rightarrow 2K(Ta, Nb)O_3 + (Fe, Mn)O + H_2O \quad (2)$$

The $K_3(Ta, Nb)O_4$ compounds formed in the first reaction are water soluble, while those formed by the second one - $K(Ta, Nb)O_3$, are not. Wang et al. (2010) reported that one of the key parameters in the successful formation of water soluble compounds is the KOH to ore molar ratio. Based on stoichiometry, reaction (1) requires molar ratios greater than or equal to 6 to completely convert Ta and Nb into water soluble compounds. Nevertheless, these considerations are not sufficient to provide a satisfactory explanation on the reaction mechanisms during the coltan roasting. Furthermore, the alkaline roasting of coltan mineral resources followed by water leaching is a developing process that requires fundamental in-depth studies on ores of different origins. Within this framework, understanding the associated kinetics and thermodynamics of the alkaline roasting of coltan ores and how water-soluble compounds are formed and ultimately high Ta and Nb extraction levels are reached, is a key requirement for the successful industrial deployment of the process.

Within the above context, the current work investigates the kinetics during potassium hydroxide (caustic potash) roasting of a coltan bearing ore from the Numbi deposit in South Kivu, the Democratic Republic of the Congo (DRC). The differences in the solubility properties between the resulting Ta and Nb compounds after the roasting are used to delineate and explain the different degrees of Ta and Nb extraction. Since caustic potash becomes fluid during roasting, the KOH-mineral particle reaction could be regarded as a solid–liquid reaction to which a shrinking core model can be applied. A pre-concentration using magnetic separation is involved in order to enrich the coltan minerals from the rest accompanying gangue, remove deleterious impurities and optimise roasting agent consumption. The thermodynamic aspects of the coltan roasting are also discussed in order to figure out the chemical reactions which are thermodynamically possible but could impede metals recovery. The examined roasting parameters involve KOH to ore mass ratio, ore particle size and operational temperature.

2. Materials and methods

2.1. Materials

A representative sample of a coltan ore (25 kg) was collected at the Numbi deposit located in the South Kivu province (DRC). The ore was dried and screened on a 2 mm sieve and the resulting coarse fraction was crushed by a roll crusher to a particle size below 2 mm. The resulting material was homogenized and a subsample (500 g) was collected by using a riffle divider. This sample was further pulverized using a ring mill and delivered for characterisation.

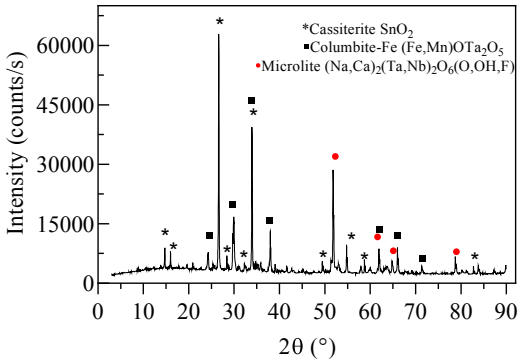

Fig. 1. XRD pattern of the ROM coltan ore.

Potassium hydroxide of analytical grade (86% w/w) provided by MERCK was used for the roasting tests, while distilled water was used for the aqueous leaching of the roasted products.

2.2. Ore characterisation

The ore samples were characterized using XRF, PIXE, ICP-AES, XRD and SEM-EDS techniques. Multi-elemental XRF analysis was performed using a BRUKER S8 TIGER system with the results shown in Table 1 indicating Sn, Ta, Nb and Ti as main metals with economic grades.

Following the indispensable digestion steps, the same sample has been subjected to Ta and Nb analysis by ICP-AES (Varian Liberty 100) which indicated that the ore contains 9.62% Ta and 4.05% Nb. A non-destructive quantitative elemental analysis, namely PIXE (particle induced X-ray emission) technique was also used to bring reconciliation of the chemical composition and increase the robustness of analytical data. This technique offers the advantage of analysis without the necessity of time consuming digestion, and by minimizing the error resulting from sample preparation (Zeman et al, 2019). The PIXE analysis was carried out by the means of a PIXE-SIAM platform, using two detectors SSD and RX LEGe. Each of the detectors was equipped with a magnetic filter to stop the *retro*-diffused particles. The average of the results provided by the two detectors were considered. These assays indicated that the ore contains 9.88% Ta and 4.75% Nb, values quite close to those obtained by the ICP-AES.

X-ray diffraction analysis was performed using a Bruker D8-ECO diffractometer, with CuK_αradiations (λ = 1,9373 Å). To this end, the respective sample was pulverized before being scanned between 5 and 75° 2θ at a speed of 0.02°2θ per second. The identification of all minerals from the XRD patterns was done with a Panalytical Xpert suite and WebPDF4 + ICDD relational database. The X-ray diffraction confirms the presence of cassiterite as a major mineral phase of the ore - Fig. 1. Ta and Nb are found mainly in the form of coltan and microlite. The other useful minerals are ilmenite and rutile while gangue minerals are represented by quartz, andalusite and muscovite.

A second subsample of the ore ground at 80% passing 75 μm was used to fabricate polished sections, following an established procedure (Bouzahzah et al., 2015). The ground sample was mixed with a viscous phase consisting of Araldite (epoxy resin) and carbon black (Printex XE 2). The obtained section was polished using GR abrasive disks with different finesses (1000–4000 μm) and finally with a diamond

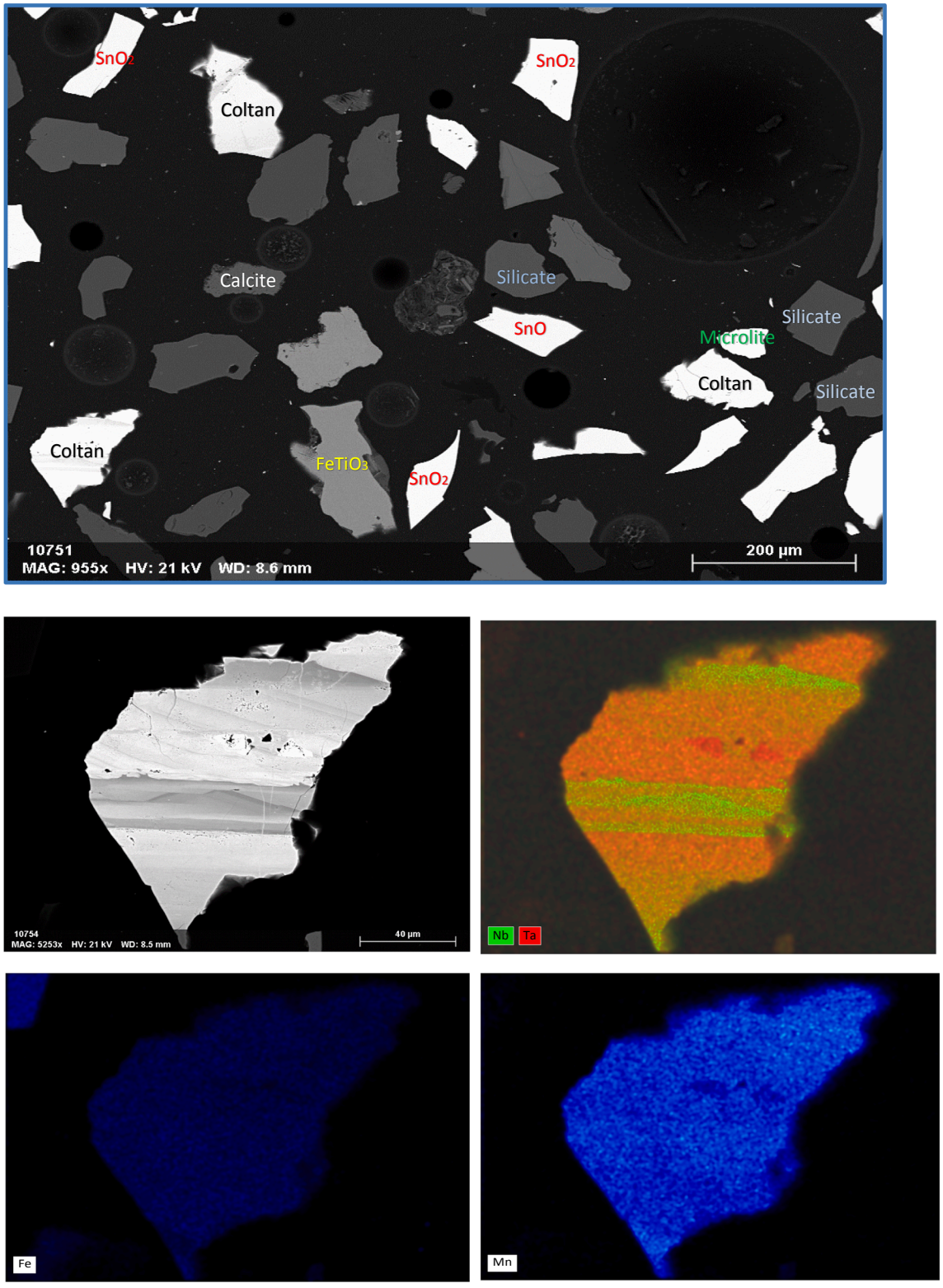

Fig. 2. BSE view of the coltan ore with major mineral phases – image above and EDS mapping for Nb, Ta, Fe nd Mn - four images below.

suspension (1PS-1MC) consisting of 1 µm sized particles in methanol as solvent. Afterwards, the interest area of the polished sections was metalized and enclosed with a silver bridge prior to be carbonized inside a Bolzers MED evaporator. The thus obtained polished sections were subjected to an automated mineralogy analysis using a ZEISS (Sigma 300) SEM-EDS system. The system is equipped with two Bruker XFlash 6I30 X ray energy dispersion spectrometers (EDS). The SEM-EDS analyses were carried out using a probe current of 2.3 nA with an accelerating voltage of 20 kV at a working distance of 8.5 mm. The obtained BSE images pictured in Fig. 2 indicated coltan, microlite and wodginite as main Ta and Nb carrying minerals. The rest minerals being present include cassiterite, ilmenite, rutile, wolframite, with quartz, andalusite, silicates and muscovite being also identified as gangue phase.

Table 2
Metallurgical balance after magnetic separation of the ground ore.

Fractions	Yield, %	Ta (%)	Nb (%)	Sn (%)
Magnetic	37.6	18.86	8.50	10.02
Non-magnetic	62.4	4.05	1.37	43.56
Feed	100	9.62	4.05	30.95

2.3. Equipment

A ball mill (Magotteaux) was used to grind the ore to 80% passing 75 μm. A high intensity magnetic separator (Carpco CC WHIMS, 850 mT) operated at field intensity of 0.85 T was used to separate coltan and cassiterite. A 500 mL borosilicate batch reactor fitted with a teflon stirrer was used for the water leaching and a 100 mL ceramic crucible was employed as a roasting vessel. The roasting was done inside a muffle furnace (Bouvier) operating between 25 and 1300 °C (±2°C) at a programmable heating rate of 10 °C/min. The temperature was monitored and controlled by means of a proportional-integral-derivative (PID) system and a thermocouple inside the furnace.

2.4. Magnetic separation

The magnetic separation aimed to separate coltan from cassiterite was realized using an ore pulp at 25% solids. The latter was prepared by wet milling of about 10 kg crushed ore to 80% passing 75 μm and using 1 kg of the ground pulp as a feed for the high intensity magnetic separation. The fractions resulting from the magnetic separation were filtered and the recovered solids left to dry in an oven and weighed. Each fraction was then assayed by an ICP-AES to establish a metallurgical balance given in Table 2.

The results shown in Table 2 enable to conclude that about 88% of the Sn bearing cassiterite could be separated from the coltan, thus bringing Ta and Nb recoveries of 73.7% and 78.9% respectively. As a consequence, about 26% of Ta and 21% of Nb remained entrained in the non-magnetic fraction. These proportions, as shown by the SEM images and the EDS spectra in Fig. 3, correspond well to the Ta and Nb present mainly in the microlite and to a lesser extent in the wodginite. It is obvious that the microlite does not contain iron which could impart magnetic properties to this mineral. The presence of wodginite in the non-magnetic fraction could be due to the weak magnetic susceptibility of some ore particles in which tin largely dominates the mineral matrix.

2.5. Roasting and leaching procedures

The roasting and aqueous leaching procedures for this study were adapted from those described in previous investigations on roasting of similar ore (Tathavadkar et al., 2001; Escudero-Castejon et al., 2016; Parirenyatwa et al., 2016). The experiments were conducted in duplicate using two analytical techniques for the solid residues assay namely an ICP-AES and PIXE, and the mean values are reported. Roasting was realized on 10 g of magnetic concentrate sample placed inside a 100 mL ceramic crucible. A predetermined amount of KOH was added to form the respective KOH/ore mass ratio and the mixture was introduced inside the muffle furnace. Once the pre-set temperature was reached, roasting commenced. Upon the required time elapsing, the roasted product was cooled down to room temperature and prepared for aqueous leaching. Each batch consisted of leaching 35 g roasted material in 400 mL water for two hours. Upon leaching completion, the unreacted residue and the pregnant leach solution (PLS) were separated by filtration. The residue was thoroughly washed with distilled water and then dried in an oven at 65 °C for 24 h. The resulting filtrates and solids were analysed by ICP-AES or PIXE to calculate leaching recovery as follows:

$$\text{leaching recovery} = \left(1 - \frac{Mr}{Mi}\right) \times 100 \quad (3)$$

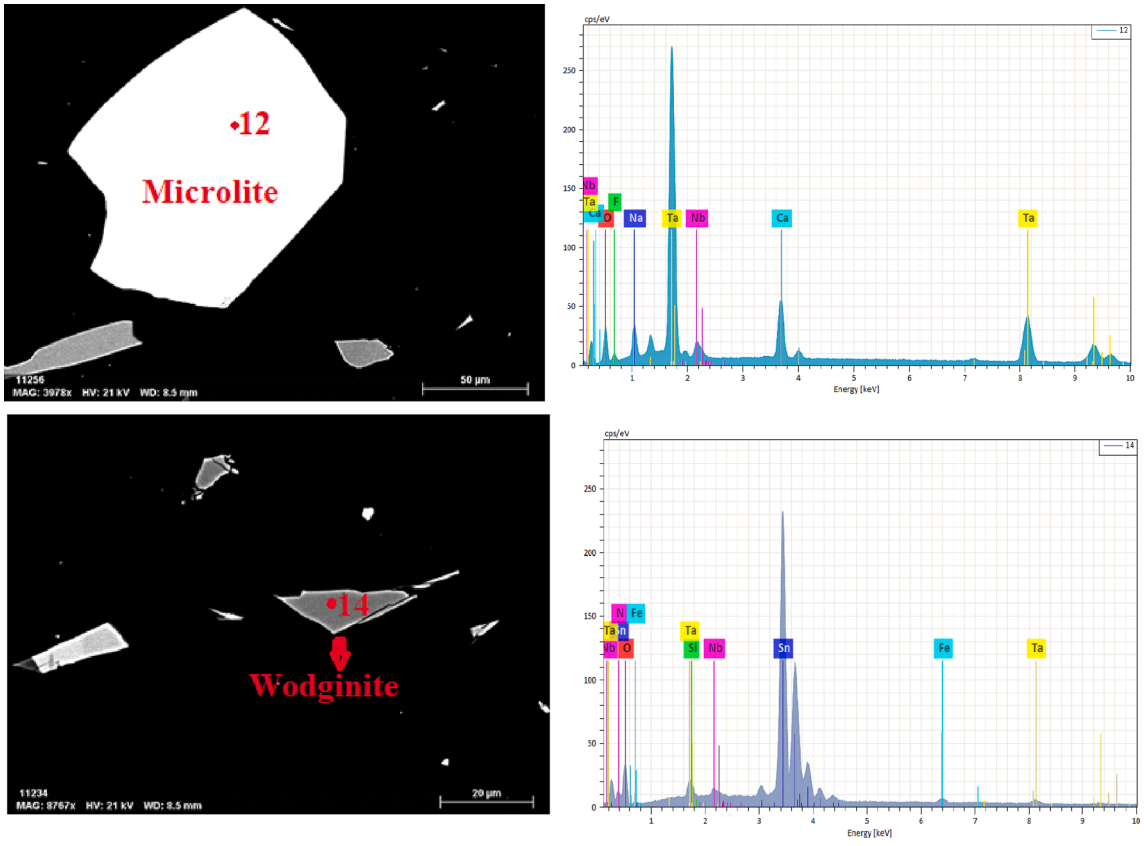

Fig. 3. Scanning electron microscopy images (left) with corresponding EDS spectra of Ta and Nb bearing minerals (right) entrained inside the magnetic fraction.

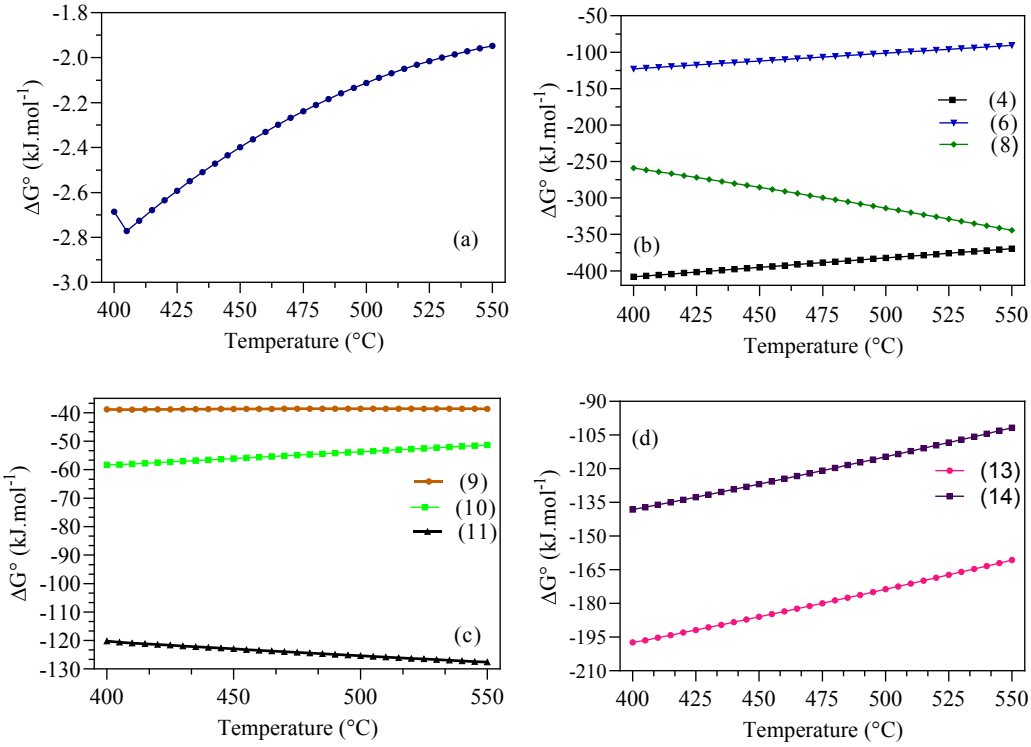

Fig. 4. Plot of Gibbs free energy against temperature: (a) reaction (5), (b) reactions (4), 6 and 8, (c) reactions 9–11 and (d) reactions 12–13.

where, Mr is the calculated mass of the metal in the leaching residue and Mi is the calculated mass of the metal in the magnetic concentrate before roasting. It is assumed, that the Ta and Nb leached out from the roasted ore correspond well to the amount of Ta and Nb converted into water-soluble compounds.

3. Results and discussions

3.1. Thermodynamics considerations

Since as a rule, coltan bearing ores are accompanied by impurities such as Fe, Mn, Sn, Si, Al, and Ti present as oxides, several side chemical reactions could be anticipated during the caustic potash roasting. The principles ones are illustrated below:

$$FeO_{(s)} + O_{2(g)} \rightarrow 2Fe_2O_{3(s)} \quad (4)$$

$$Fe_2O_{3(s)} + 2KOH_{(s)} \rightarrow 2KFeO_{2(s)} + H_2O_{(g)} \quad (5)$$

$$2MnO_{(s)} + O_{2(g)} \rightarrow 2MnO_{2(s)} \quad (6)$$

$$MnO_{2(s)} + 2KOH_{(s)} \rightarrow K_2MnO_{3(s)} + H_2O_{(g)} \quad (7)$$

$$TiO_{2(s)} + 2KOH_{(s)} \rightarrow K_2TiO_{3(s)} + H_2O_{(g)} \quad (8)$$

$$Al_2O_{3(s)} + 2KOH_{(s)} \rightarrow 2KAlO_{2(s)} + H_2O_{(g)} \quad (9)$$

$$4SiO_{2(s)} + 2KOH_{(s)} \rightarrow K_2Si_4O_{9(s)} + H_2O_{(g)} \quad (10)$$

$$SiO_{2(s)} + 2KOH_{(s)} \rightarrow K_2SiO_{3(s)} + H_2O_{(g)} \quad (11)$$

$$SnO_{2(s)} + 2KOH_{(s)} \rightarrow K_2SnO_{3(s)} + H_2O_{(g)} \quad (12)$$

$$Ta_2O_{5(s)} + 2KOH_{(s)} \rightarrow 2KTaO_{3(s)} + H_2O_{(g)} \quad (13)$$

$$Nb_2O_{5(s)} + 2KOH_{(s)} \rightarrow 2KNbO_{3(s)} + H_2O_{(g)} \quad (14)$$

In order to decrypt and theoretically understand the mechanisms involved in the investigated alkaline roasting, a thermodynamic study on the spontaneity of these reactions was considered as essential. The standard Gibbs free energy change of each reaction was calculated using the HSC Chemistry 7.0 software (Roine, 2009) within the temperature range of 400–550 °C. The computed values are plotted against the temperature and shown in Fig. 4. It has to be noted, that the standard Gibbs free energy change for reactions (7) and (12) is not plotted as data on some chemical species were not available in the database.

A perusal of the results in Fig. 4 suggests that all chemical reactions are thermodynamically possible within the considered temperature range. This fact undoubtedly could lead to an overconsumption of KOH during roasting, thus reducing its availability for Ta and Nb conversion as water-soluble compounds.

The KOH roasting in an oxidizing atmosphere leads to an oxidation of Fe^{+2} (FeO) into Fe^{+3} (Fe_2O_3). The formed Fe_2O_3 can also react with KOH according to reaction (5) and form $KFeO_2$. Tathavadkar et al. (2003) reported that the high melting point of sodium aluminate ($NaAlO_2$) and ferrite ($NaFeO_2$) during the alkaline roasting induces changes in the chemical and physical properties of the liquid phase. Since K, and Na are both alkali metals with similar behaviour, these observations are also valid during the potash ore roasting. Moreover, the potassium silicate compounds decrease the activity of the alkali metal ions (Na^+, K^+) and increase the viscosity of the liquid phase (Tathavadkar et al., 2003; Escudero-Castejon et al., 2016), which from its side tends to inhibit the reactions responsible for yielding the desired water-soluble compounds.

The side reactions (13) and (14) forming undesirable compounds of Ta and Nb could be depicted in Fig. 4d. They are favourable under the considered temperature range, however they become less spontaneous with increased temperature. Therefore, raising the roasting temperature should be pursued in order to avoid their formation.

3.2. Roasting and leaching results

3.2.1. Effect of KOH/ore mass ratio

The effect from the alkaline agent/ore mass ratio was studied through performing roasting experiments at five different ratios: 0.8/1,

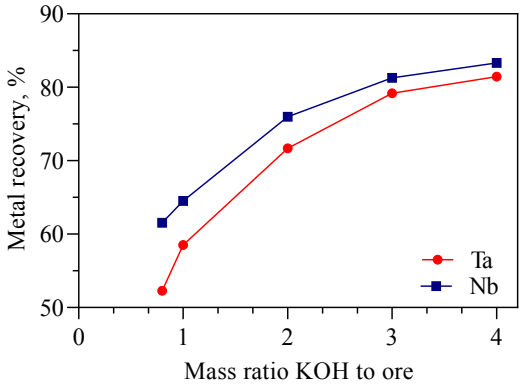

Fig. 5. Effect of KOH to ore ratio on Ta and Nb recoveries (roasting temperature: 550 °C, particle size: d_{80} = 75 μm).

Table 3
Nb and Ta content of the studied granulometric fractions.

Particle size range (μm)	Nb (%)	Ta (%)
−150 + 105	6.82	14.93
−105 + 75	8.14	17.77
−75 + 45	11.29	20.23

1/1, 2/1, 3/1, 4/1. These ratios were chosen based on the thermodynamics considerations shown in Section 3.1. The potassium hydroxide can be consumed by alumina and silica to form potassium aluminates and potassium silicates, as shown in Fig. 4c. By taking into account the alumina, the silica and the other impurities the ore contains, it becomes necessary to increase the amount of added KOH above the stoichiometric one. Fig. 5 shows the results regarding the effect of KOH/ore variation on the Ta and Nb recoveries.

It can be seen from Fig. 5, that the increase in the KOH/ore ratio is accompanied by an increase in Ta and Nb recoveries. The higher KOH/ore mass ratio renders the mixture less viscous, thus facilitating the Ta and Nb transformation by the KOH towards the targeted water-soluble species. Moreover, the higher KOH/ore mass ratio increases the availability of potash for the desired roasting reaction compensating the presence of gangue minerals as well. For this reason, the KOH mass ratio must be optimised to secure high recoveries of Ta and Nb during roasting. It is worth noting, that Ta and Nb recoveries do not increase dramatically when the KOH/ore mass ratio increases over 3/1. Moreover, a further increase in KOH/ore mass ratio should be avoided due to cost reasons and viscosity issues complicating the solid–liquid separation downstream. Therefore, the effect from particle size and temperature on coltan roasting were studied at fixed KOH/ore ratio of 3/1.

3.2.2. *Effect of particles size*

The particle size of the solid substrate is an important parameter when performing kinetic studies of solid–liquid reactions. To this end, the coltan rich magnetic concentrate was dry sieved and classified into three granulometric fractions as follows: −150 + 105 μm, −105 + 75 μm, −75 + 45 μm. They were used accordingly to investigate the effect of particle size on Ta and Nb recoveries. The Ta and Nb content in each fraction is presented in Table 3.

The effect from particle size on the metals recovery was studied at roasting temperature of 550 °C and KOH/ore mass ratio of 3/1 and the respective results are shown in Fig. 6.

It can be seen from Fig. 6, that both Ta and Nb recoveries increase with decrease in ore particle size, which may be explained by the fact that the smaller the ore particles, the larger their specific surface area and the higher their reactivity towards KOH is. After 10 min of roasting ore with particle size range −75 + 45 μm, about 72% of Nb and 66% of Ta are leached out by water. After this period, the Ta and Nb recovery curves are reaching a plateau, which may be explained by the fact that the mixture becomes more viscous due to the almost complete water

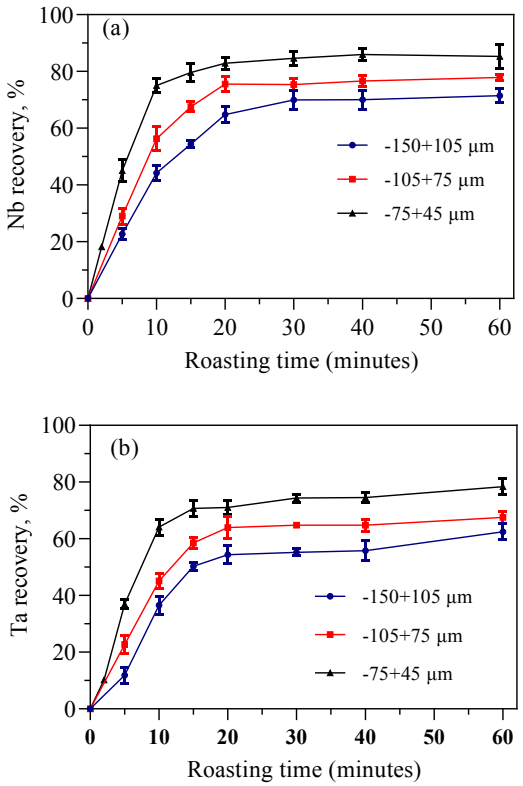

Fig. 6. Effect of particle size on the recovery of Nb (a) and Ta (b).

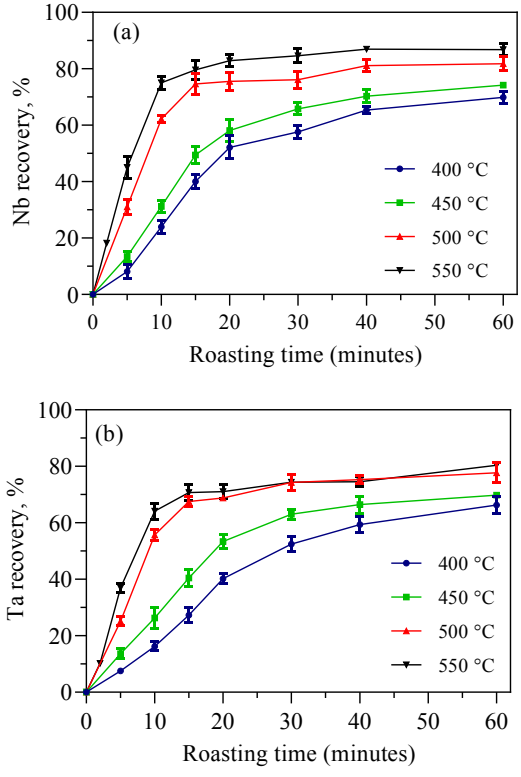

Fig. 7. Effect of roasting temperature on Nb (a) and Ta (b) recoveries following water leaching.

Table 4
Apparent rate constants and model correlation coefficients for the three granulometric fractions.

Element	Particle size range (μm)	$1-(1-\hat{I}\pm)^{\frac{1}{3}}$		$\left(1-(1-\alpha)^{\frac{1}{3}}{}^{2}\right)$		$1-\frac{2}{3}\hat{I}\pm-1-(1-\hat{I}\pm)^{\frac{2}{3}}$	
		k_c (min^{-1})	R^2	k_j (min^{-1})	R^2	k_d (min^{-1})	R^2
Nb	(−75 + 45)	0.0367	0.9988	0.0120	0.8842	0.0092	0.9087
	(−105 + 75)	0.0202	0.9560	0.0066	0.9486	0.0051	0.9512
	(−150 + 105)	0.154	0.9862	0.0038	0.9376	0.0032	0.9538
Ta	(−75 + 45)	0.0281	0.9905	0.0071	0.8854	0.0058	0.9020
	(−105 + 75)	0.0158	0.9725	0.0040	0.9490	0.0033	0.9601
	(−150 + 105)	0.0124	0.9642	0.0026	0.9203	0.0022	0.9273

evaporation, which adversely affects the reactions between the ore particles and the KOH.

3.2.3. Effect of roasting temperature

The roasting temperature effect on Ta and Nb recoveries was investigated in the range of 400–550 °C. The remaining process conditions were kept unchanged: i.e. the ore granulometry range was −75 + 45 μm and the KOH to ore mass ratio − 3/1. The results from this experimental trial are shown in Fig. 7.

From the results shown in Fig. 7, it can be seen that the temperature plays an important role on the roasting kinetics and leachability of Ta and Nb. A temperature increase from 400 to 550 °C apparently accelerates the transformation of Ta and Nb to water soluble compounds and increases their recovery during the aqueous reaction stage. About 72% of Nb and 66% of Ta were water leached after only 10 min when the material was roasted at 550 °C, while at 400 °C, Nb and Ta were water leached to a maximum of 25.7% and 18.3%.

It could be noted, that although having similar properties, the two studied metals do exhibit different behaviours during the alkaline roasting. The recovery of Nb is always higher than that of Ta and this was observed during all the experiments. A plausible explanation of this phenomenon could go back to Section 3.1, where the thermodynamic calculations have suggested that undesirable reactions yielding water-insoluble compounds are far more likely to happen in the case of Ta than of Nb.

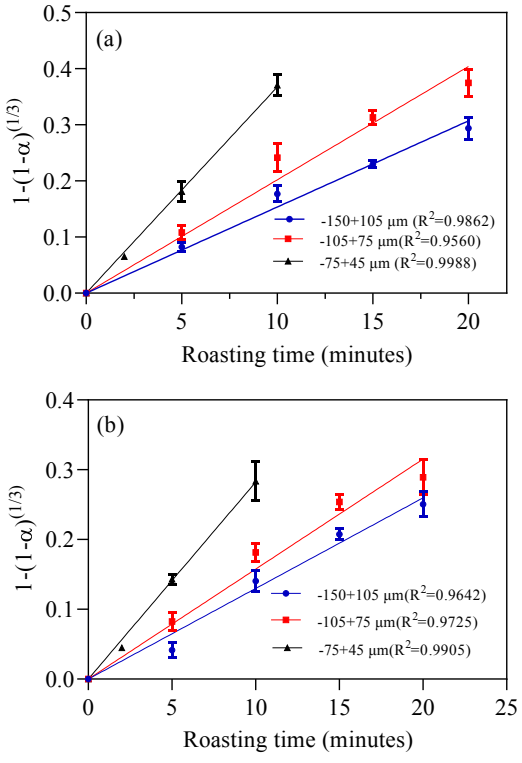

Fig. 8. Plot of $1-(1-\alpha)^{\frac{1}{3}}$ vs. roasting time for the three particle size ranges, Nb (a), Ta (b).

3.3. Reaction kinetics considerations

3.3.1. Kinetic models

Several models describing solid–liquid reactions have been proposed to investigate the rate-controlling steps in hydrometallurgy. These models are widely discussed in the literature (Levenspiel, 1999; Liddell, 2005) and their application proved useful in previous studies dealing with mineral ores roasting (Tathavadkar et al., 2001; Antony et al., 2006; Liu et al., 2017). Assuming that a coltan mineral particle has a spherical shape, three models (based on the shrinking core theory) are tested here and compared to identify the rate-controlling step during KOH roasting. Their descriptive equations could be respectively presented as follows:

$$1-(1-\alpha)^{\frac{1}{3}}=\frac{k_0 m_s C_A}{\rho_s a r_0}=k_c t \tag{15}$$

$$1-\frac{2}{3}\alpha-(1-\alpha)^{\frac{2}{3}}=\frac{2m_s D C_A}{\rho_s a r_0^2}=k_d t \tag{16}$$

$$\left(1-(1-\alpha)^{\frac{1}{3}}{}^{2}\right)=k_{jt} \tag{17}$$

where α is the leached fraction of the metal (Ta or Nb), $k_0$is the reaction constant, m_s is the molecular mass of the roasted ore ($kg.mol^{-1}$), C_A is the potassium hydroxide concentration ($mol.m^3$), D is the diffusion coefficient, a is the stoichiometry coefficient, r_0 is the initial radius of the ore particle (m), t is the reaction time (minutes), ρ_s is the density of the ore particle ($kg.m^{-3}$) and k_c, k_d and k_{jt} are the apparent rate constants for equations (15), (16) and (17), respectively. Eq. (15) (Spencer and Topley equation) represents a chemically controlled reaction, while equation (16) (Ginstling and Brounshtein equation) represents an external diffusion controlled reaction. Eq. (17) (Jander equation) represents a

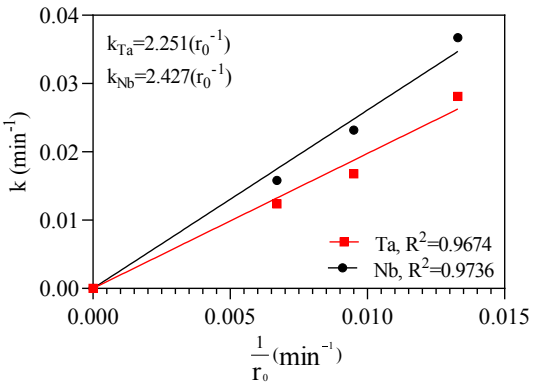

Fig. 9. Plot of reaction rate constant vs $1/r_o$ for Ta and Nb.

diffusion controlled process as well, but in this model, the diffusion occurs between two flat-planes contacting solids that create a product layer between them.

When applying the kinetic models, an assumption is made that only data for which the kinetics is deemed sufficiently fast are considered. Table 4 compares the correlation coefficients and the respective apparent reaction rate constants for the three models at the studied particle size ranges. Looking at the data, one could clearly derive that the model described by Eq. (15) is the most suitable one for the case of coltan roasting.

Further on, Fig. 8 indicates that the mean values for the apparent rate constant correlate well with the selected model, thus meaning that the caustic potash roasting of coltan is governed by a chemical reaction.

Generally, the rate constant of a chemically controlled reaction is inversely proportional to the initial radius of the ore particle, while in those controlled by diffusion it is inversely proportional to the square of the initial radius of the particle (Zhou et al, 2005a; Yang et al, 2013). Based on the apparent rate constants corresponding to the slopes of the trend lines shown in Fig. 8, one could derive Fig. 9. It illustrates that the apparent rate constant lies in close correlation with the inverse of the initial particle radius. This fact reaffirms the assumption that the caustic potash roasting of the tested coltan ore is controlled by a chemical reaction.

3.3.2. Apparent activation energy

The temperature dependence of the likelihood for a solid–liquid reaction is often used to estimate its apparent activation energy. Generally, the effect from temperature is more pronounced in the case when the process is controlled by a chemical reaction than when governed by reagents diffusion. As can be seen in Fig. 10, the kinetics is the fastest during the first 10 min at temperature of 550 °C, and obviously slows down when the temperature is maintained at 400 °C.

For a process controlled by a chemical reaction and dependent on temperature, the activation energy can easily be deduced from the following Arrhenius equation:

$$k_1 = A\exp(-\frac{Ea}{RT}) \quad (19)$$

where A is the pre-exponential factor, E_a is the apparent activation energy (kJ.mol^{-1}), R is the universal gas constant (8.314 kJ.mol^{-1}.K^{-1}), T is the temperature (K).

The mathematical transformation of Eq. (19) results in the Eq. (20) below:

$$\ln k = \ln A - \frac{E_a}{R}(\frac{1}{T}) \quad (20)$$

The apparent rate constants (k_c) for each of the tested temperature ranges have been estimated from the slopes of the fitted lines pictured in Fig. 10. The relationship between the logarithm of these apparent rate constants and the inverse of temperature are shown in Fig. 11. The activation energy can be calculated as 40.9 and 46.1 kJ.mol^{-1} for Nb and Ta respectively.

The value of the apparent activation energy can also be used to

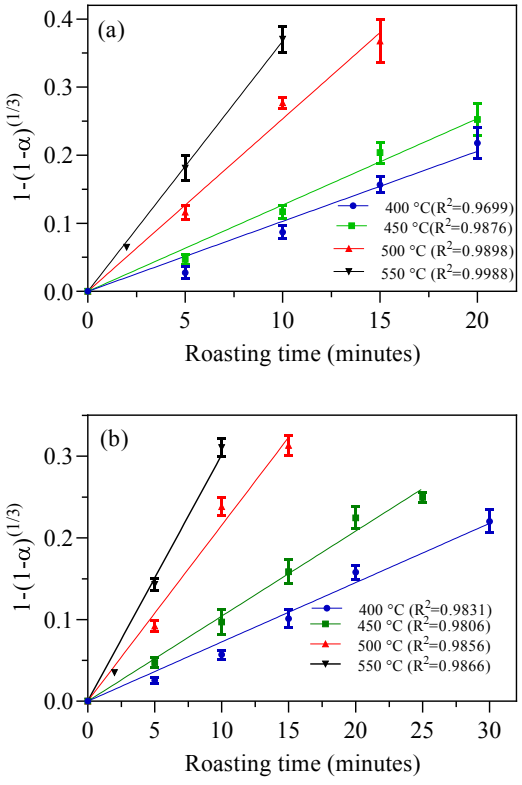

Fig. 10. Plot of $1-(1-\alpha)^{\frac{1}{3}}$ against roasting time at various temperatures (particle size: −75 + 45 μm, KOH/ore mass ratio: 3/1).

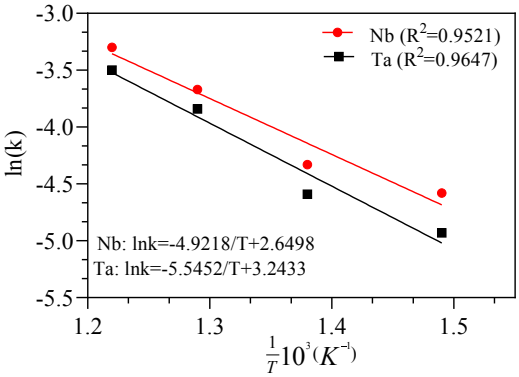

Fig. 11. Plot of ln(k) against inverse of temperature.

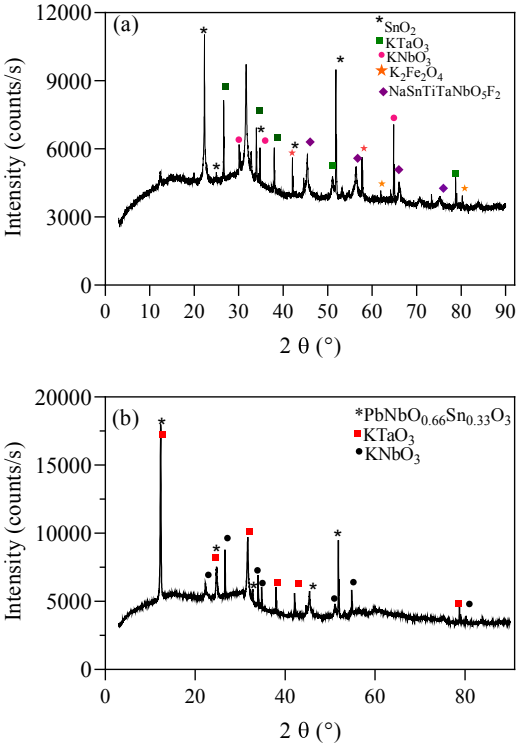

Fig. 12. XRD pattern of the leached residue: 10 min roasting - a, 1 h roasting - b; (KOH/ore ratio: 3/1, roasting temperature: 550 °C).

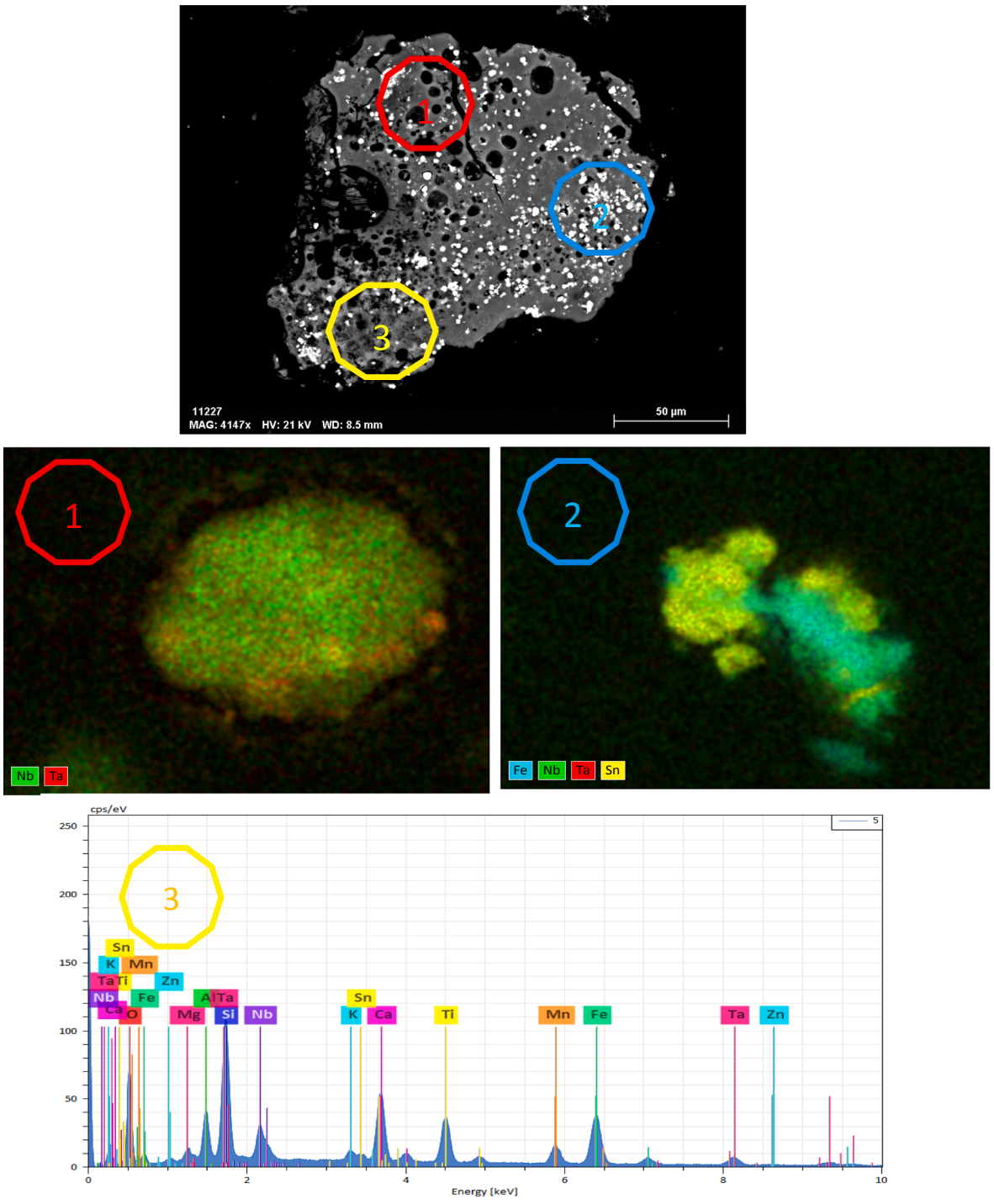

Fig. 13. SEM view of leaching residue (upper image) and close view of characteristic spots, with EDS mapping for Nb-Ta (1) and Fe-Nb-Ta-Sn (2) and EDS spectra at position 3.

predict the rate-controlling step of the reaction. For a diffusion-controlled process, the activation energy is generally less than 40 $kJ.mol^{-1}$ and is often around 21 $kJ.mol^{-1}$, but is higher than 40 $kJ.mol^{-1}$ for a process controlled by a chemical reaction (Levenspiel, 1999). However, it has been previously shown, that the activation energy does not precisely predict the rate-controlling step. In our study, the calculated activation energies for Nb (40.9$kJ.mol^{-1}$) and Ta (46.1 $kJ.mol^{-1}$) confirm that the coltan roasting process is controlled by a chemical reaction. The identified rate-controlling step for Nb confirms the findings reported by Yang et al. (2013) on caustic soda roasting of Ta-Nb ore, but the value for the activation energy obtained in our case is lower than the one reported by Yang et al. (2013). This difference could be due to variations in the mineralogy of the tested ores and the envisaged operational conditions, in particular particle size, type of alkaline agent and its ore addition ratio.

3.4. Leaching residue characterization

The residue after leaching was submitted to XRD and SEM-EDS characterization in order to identify the remaining Ta and Nb bearing phases. However, the fact that the residues were almost amorphous brought some difficulties during the XRD quantification of the available Ta-Nb bearing phases, leading to $KTaO_3$ and $KNbO_3$ being only distinguished - Fig. 12. These two compounds are known to be water-insoluble and have been likewise identified in previous studies (Wang et al., 2009, 2010; Berhe et al., 2018).

Fig. 13 depicts some characteristic morphological features of the obtained residue after roasting and water leaching along with the elemental composition at selected spots.

The images shown in Fig. 13 suggest that two main phases could be distinguished inside the water leached residues: a partially reacted coltan bearing phases and a complex solid solution resulting from roasting. It can be seen that the surface of the ore particles was eroded by the molten potassium hydroxide and a porous surface has emerged during roasting – Fig. 13-2. The EDX mapping (Fig. 13-3) indicates that the different metals associated with the input sample tend to form a solid solution which is refractory to water leaching. These observations are in close agreement with findings reported in previous studies (Escudero-Castejon et al, 2016; Parirenyatwa et al., 2016) and conducted on an alkaline roasting of an ore containing impurities such as silica, alumina, and iron oxides.

4. Conclusions

The optimal roasting process parameters and the associated kinetics when converting Ta and Nb met in a coltan ore into water leachable compounds have been investigated. The ore pre-treatment by magnetic separation was able to remove about 88% of the contained cassiterite and thus to yield an upgraded coltan concentrate with nearly 19% Ta and 8.5% Nb. The roasting experiments demonstrated that operational parameters such as KOH-ore mass ratio, particle size and temperature do influence strongly the formation of water soluble compounds of K_3TaO_4 and K_3NbO_4 type. Ta and Nb recoveries during the water leaching stage increase with the decrease in ore particle size and with the increase in KOH-ore ratio and roasting temperature. Relatively narrow particle size range ($-75 + 45$ μm), reagent/ore mass ratio of 3/1 and roasting during 1 h at 550 °C were required to guarantee satisfactory recovery of Ta and Nb in the water lixiviant. Under these conditions, about 87% of Nb and 80% of Ta were rendered water leachable, giving a pregnant leaching solution suitable for down-stream treatment by solvent extraction (ca. 4.6 g/L Ta, 2 g/L Nb, pH 13). The major impurities accompanying the coltan like Fe and Mn have been leached to an extent less than 10%.

The kinetic study suggested that coltan roasting is a chemical reaction controlled process. The activation energies have been calculated as 40.9 and 46.1 $kJ.mol^{-1}$ for Nb and Ta respectively. These values are in accordance with literature data reported for a process controlled by a chemical reaction.

Declaration of Competing Interest

None.

Acknowledgements

The work was supported by the ARES Academy (Belgium) within the PRD 2019 ARES-CCD project. A. Shikika would like to acknowledge the additional funding from the Faculty of Applied Sciences (University of Liège). Prof. Fr. Hatert, Dr H. Bouzahzah and Mr. J. Colaux are gratefully acknowledged for their outstanding support with the mineralogical inspection.

References

Agulyansky, A., 2004. The chemistry of tantalum and niobium fluoride compounds. Elsevier, Amsterdam.
Allain, E., Kanari, N., Diot, F., Yvon, J., 2019. Development of a process for the concentration of the strategic tantalum and niobium oxides from tin slags. Miner. Eng., 134, pp. 97-103, https://doi.org/10.1016./j.mineng.2019.01.029.
Antony, M.P., Jha, A., Tathavadkar, V., 2006. Alkali roasting of Indian chromites ores: thermodynamic and kinetics considerations. IMM Trans., Sect. C: Mineral Process. Extractive Metall. 115 (2), 71–79. https://doi.org/10.1179/174328506X109086.
Berhe, G.G., Velasquez, D.A., Bogale, T., Abubeker, Y., Girma, W., 2018. Decomposition of the Kenticha mangano-tantalite ore by HF/H_2SO_4 and KOH fusion. Physicochem. Probl. Miner. Process. 54 (2), 406–414. https://doi.org/10.5277/ppmp1840.
Bouzahzah, H.; Benzaazoua, M., Mermillod-Blondin, R., Pirard, E., 2015. A novel procedure for polished section preparation for automated mineralogy avoiding internal particle settlement. In: 12th International Congress for Applied Mineralogy (ICAM). 10-12 August 2015, Istanbul, Turkey.
Brocchi, E.A., Moura, F.J., 2008. Chlorination methods applied to recover refractory metals from tin slags. Miner. Eng. 21 (2), 150–156. https://doi.org/10.1016/j.mineng.2007.08.011.
Escudero-Castejon, Sanchez-Segado, S., Parirenyatwa, S., Jha, A., 2016. Formation of chromium containing molten salt phase during roasting of chromite ore with sodium and potassium hydroxides. J. Manuf. Sci. Prod., 16(4), pp 215-225. https://doi.org/10.1515/jmsp-2016-0023.
Gaballah, I., Allain, E., Djona, M., 1997. Extraction of tantalum and niobium from tin slags by chlorination and carbochlorination. Metall. Mater. Trans. B: Process Metall. Mater. Process. Sci. 28 (3), 359–369. https://doi.org/10.1007/s11663-997-0102-7.pdf.
Hayes, K., Bruge, R., 2003. Coltan mining in the Democratic Republic of Congo: how tantalum using industries can commit to the reconstruction of the DRC. Fauna and Flora International, Cambridge, UK, ISBN 1-903703-10-7.
El Hazek, M.N., Mohamed, N.H., Gabr, A.A., 2019. Potash breakdown of poly-mineralized Niobium-Tantalum-Lanthanides ore material. Am. J. Anal. Chem. 10 (03), 103–111. https://doi.org/10.4236/ajac.2019.103009.
Htwe, H.H., Lwin, K.T., 2008. Study on extraction of niobium oxide from columbite-tantalite concentrate. World Acad. Sci., Eng. Technol. 46, 133–135.
Levenspiel, O., 1999. Chemical reaction engineering (Ch. 25: Fluid reactions-particles reactions, kinetics), 2nd edition. Wiley, New York. ISBN 0-471-25424-X.
Liddell, Kona C., 2005. Shrinking core models in hydrometallurgy: what students are not being told about the pseudo-steady approximation. Hydrometallurgy 79 (1–2), 62–68. https://doi.org/10.1016/j.hydromet.2003.07.011.
Liu, J., Zhai, Y., Wu, Y., Zhang, J., Shen, X., 2017. Kinetics of roasting potash feldspar in the presence of sodium carbonate. J. Central South Univ. 24 (7), 1544–1550. https://doi.org/10.1007/s11771-017-3559-9.
Mantz, W.J., 2008. Improvisational economies: coltan production in the Eastern Congo. Soc. Antropol. 16 (1), 34–50. https://doi.org/10.1111/j.1469-8676.2008.00035.x.
Moran, D., McBain, D., Kanemoto, et al., 2014. Global supply chains of coltan: A hybrid like cycle assement study using a social indicator. J. Industr. Ecol., 19(3), pp. 357-365. https://doi.org/10.1111/jiec.12206.
Parirenyatwa, Lidia, Sergio, Yotamu, Jha, 2016. Comparative study of alkali roasting and leaching of chromite ores and titaniferous minerals. Hydrometallurgy 165, pp 213-226. https://doi.org/10.1016/j.hydromet.2015.08.002.
Roine, A., 2009. Chemistry for windows: chemical reactions and equilibrium software with extensive thermodynamical database and flowsheet simulation, version 7.1, User's guide. Outokumpu research Oy, Finland. ISBN: 978-952-92-6242-7.
Tathavadkar, V.D., Antony, M.P., Jha, A., 2001. The soda-ash roasting of chromite minerals: kinetics considerations. Metall. Mater. Trans. B: Process Metall. Mater. Process. Sci. 32 (4), 593–602. https://doi.org/10.1007/s11663-001-0115-6.
Tathavadkar, V., Jha, A., Antony, M., 2003. The effect of salt-phase composition on the rate of soda-ash roasting of chromite ores. Metall. Mater. Trans. B, 2003. 34(B): p. 555-563. https://doi.org/10.1007/s11663-001-0115-6.
Wakenge, Claude Iguma, 2018. Accessing coltan mines in the Eastern Democratic Republic of Congo. Extractive industries of Congo Soc. 5 (1), 66–72. https://doi.org/10.1016/j.exis.2017.11.008.

Wang, X., Zheng, S., Hongbin, X., Zhang, Y., 2009. Leaching of niobium and tantalum from a low-grade ore using a KOH roast-water leach system. Hydrometallurgy 98 (3–4), 219–223. https://doi.org/10.1016/j.hydromet.2009.05.002.

Wang, X., Zheng, S., Hongbin, X., Zhang, Y., 2010. Dissolution behaviors of Ta2O5, Nb2O5 and their mixture in KOH and H2O system. Trans. Nonferrous Metals Soc. China (English Edition), The Nonferr. Metals Soc. China, 20(10), pp. 2006–2011. https://doi.org/10.1016/S1003-6326(09)60409-X.

Yang, X., Wang, X., Chang, W., Zheng, S., Qing, S., 2013. Decomposition of nionium ore by sodium hydroxide fusion methode. Metall. Mater. Trans. B: Process Metall. Mater. Process. Sci. 44(1), pp 45-52. https://doi.org/pdf/10.1007/s11663-012-9766-8.pdf.

Zeman, J., Ješkovský, M., Kaizer, J., Pánik, Kontul, J., Staníček, J., Povinec, P., 2019. Analysis of meteorite samples using PIXE technique. J. Radioanal. Nucl. Chem., 322, pp.1897-1903. https://doi.org/10.1007/s10967-019-06851-9.

Zhou, H., Zheng, S., Zhang, Y., Dan-qing, Y., 2005a. A kinetic study of the leaching of a low-grade niobium-tantalum ore by concentrated KOH solution. Hydrometallurgy 80 (3), 170–178. https://doi.org/10.1016/j.hydromet.2005.06.011.

Zhou, H., Zheng, S., Zhang, Y., 2005b. Leaching of a low-grade niobium-tantalum ore by highly concentrated caustic potash solution. Hydrometallurgy 80 (1–2), 83–89. https://doi.org/10.1016/j.hydromet.2005.07.006.